QUARTERLY OF APPLIED MATHEMATICS
VOLUME LIX, NUMBER 4
DECEMBER 2001, PAGES 615–635

A NONCONVEX SCALAR CONSERVATION LAW WITH TRILINEAR FLUX

BY

BRIAN T. HAYES (*Department of Mathematics, Duke University, Durham, NC*)

AND

MICHAEL SHEARER (*Center for Research in Scientific Computation and Department of Mathematics, North Carolina State University, Raleigh, NC*)

Abstract. The focus of this paper is on traveling wave solutions of the equation

$$u_t + f(u)_x = \epsilon u_{xx} + \epsilon^2 \gamma u_{xxx},$$

in which the flux function f is trilinear and nonconvex. In particular, it is shown that for combinations of parameters in certain ranges, there are traveling waves that converge as $\epsilon \to 0$ to *undercompressive shocks*, in which the characteristics pass through the shock. The analysis is based on explicit solutions of the piecewise linear ordinary differential equation satisfied by traveling waves. The analytical results are illustrated by numerical solutions of the Riemann initial value problem, and are compared with corresponding explicit results for the case of a cubic flux function.

1. Introduction.

We consider a scalar conservation law

$$u_t + f(u)_x = 0, \tag{1.1}$$

in which $f(u)$ is trilinear and nonconvex, as shown in Fig. 1. The main goal of the paper is to calculate undercompressive shock waves directly, and to analyze parameter ranges for which they exist and do not exist. The analytical results are supplemented by numerical experiments that illustrate the structure of solutions of Riemann problems, and the dependence of parameters upon each other.

An *undercompressive* shock is a discontinuous weak solution of (1.1) with the property that characteristics pass through the shock, whereas in a *compressive* shock the characteristics impinge on the discontinuity from both sides. To specify undercompressive shocks in a useful way, there must be an additional distinguishing condition. In this

Received August 18, 1998.
2000 *Mathematics Subject Classification.* Primary 35L60, 35G25.
Michael Shearer is an Adjunct Professor of Mathematics at Duke University. His research was supported by National Science Foundation grant DMS 9504583, and by Army Research Office grant DAAG55-98-1-0128.

paper, a shock wave will be considered to be γ-*admissible* if and only if it is the limit as $\epsilon \to 0$ of traveling wave solutions of the equation

$$u_t + f(u)_x = \epsilon u_{xx} + \epsilon^2 \gamma u_{xxx}. \tag{1.2}$$

In this equation, the parameter γ expresses the relative strengths of dissipation and dispersion. As in [4], there can be undercompressive shocks for $\gamma > 0$, while there are no undercompressive shocks for $\gamma \leq 0$.

Similar criteria involving both dissipation and dispersion have been studied for certain scalar equations, hyperbolic systems and systems of mixed type [2, 5, 6, 8, 10, 11, 12]. In particular, Abeyaratne and Knowles [1] studied a system of mixed type with a nonmonotone trilinear nonlinearity and admissibility defined through viscosity and capillarity corresponding to our dissipation and dispersion in (1.2). In the system case, the calculations become quite intricate, and the analysis has not been carried to completion. However, for the scalar equation of this paper, we are able to fully analyze the problem of characterizing admissible shocks, and to use this characterization to solve Riemann problems.

The results of this paper provide explicit analytical information about undercompressive shock waves that can be used to test numerical methods designed to capture or represent undercompressive shocks for more general equations or systems. The earlier analysis [6] of a cubic flux function provides another test case that is documented analytically. However, the trilinear flux function differs in several respects from the cubic case. In particular, the parameter ranges in which undercompressive shocks exist are more subtle for the trilinear flux, and the proofs are more intricate, though elementary.

In Sec. 2, we reduce a general, nonconvex, trilinear flux to a one-parameter function and describe the elementary waves that will appear in the solution of the Riemann initial value problem. Section 3 contains our main results on undercompressive shock waves. Specifically, we show that in certain parameter ranges there always exist undercompressive shocks, while in the complementary ranges, undercompressive shocks do not exist. We conclude this section by discussing the explicit solution of the algebraic equations for the traveling waves corresponding to undercompressive shocks.

The Riemann problem is studied in Sec. 4; here we describe the solution, showing the particular wave combinations in the (u_L, u_R)-plane, in four parameter regimes. We conclude in Sec. 5 with the numerical solution of the Riemann problem for the partial differential equation (1.2). As in [3, 4], we use a high-order flux discretization, and obtain excellent agreement with the analytical Riemann solutions of Sec. 4.

2. Preliminaries. In this section, we first show that the one-parameter family of flux functions, displayed in Fig. 1, contains all the generality of an arbitrary, trilinear, nonconvex flux. We then examine elementary waves for Eq. (1.1) . The structure of these waves is somewhat degenerate because the nonlinearity is piecewise linear rather than smooth. In Sec. 3, we discuss which of these waves should be considered admissible.

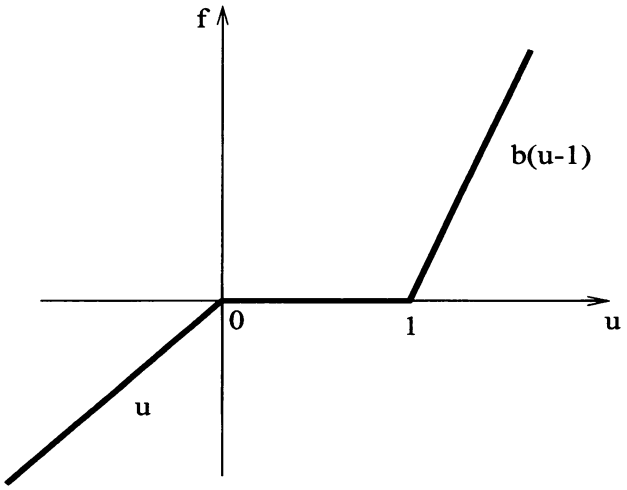

FIG. 1. The reduced trilinear flux function, shown for $b > 1$

a. *Reduction to a one-parameter trilinear flux.* Consider a general trilinear nonconvex flux function

$$f(u) = \begin{cases} b_- u & \text{if } u \le 0, \\ b_0 u & \text{if } 0 < u < a, \\ b_+(u-a) + b_0 a & \text{if } u \ge a, \end{cases} \tag{2.1}$$

with $a > 0$ and $b_0 < b_\pm$. First note that we have taken $f(0) = 0$ and $f(u)$ linear for $u < 0$ without loss of generality, since translations of u or f by a constant leave equation (1.2) unchanged. Moreover, although we have $b_0 < b_\pm$, we could equally well reverse this inequality on the coefficients. Next, we may take $b_0 = 0$, by replacing $f(u)$ by $f(u) - b_0 u$, and using a moving coordinate frame with speed b_0; i.e., replace x by $x - b_0 t$. The next normalization is to reduce to the case $a = 1$. This is achieved by scaling u by a: replace u by $w = u/a$, and $f(u)$ by $g(w) = f(aw)/a$. Then effectively, b_- is unchanged, and $b_+(u-a)$ becomes $b_+(w-1)$. Finally, we scale g to set $b_- = 1$: replace $g(w)$ by $g(w)/b_-$. Then t, ϵ, b_+ and γ must be rescaled also:

$$t' = t/b_-, \qquad \epsilon' = \epsilon b_-, \qquad b = b_+/b_-, \qquad \gamma' = \gamma/b_-.$$

Then (dropping the primes), the equation reduces to (1.2) with flux function given by (see Fig. 1):

$$f(u) = \begin{cases} u & \text{if } u \le 0, \\ 0 & \text{if } 0 < u < 1, \\ b(u-1) & \text{if } u \ge 1. \end{cases} \tag{2.2}$$

b. *Elementary waves.* We now consider elementary waves for Eq. (1.1). These waves will be used to solve Riemann problems, which are initial value problems for Eq. (1.1)

with initial data consisting of two constants:

$$u(x,0) = \begin{cases} u_L & \text{if } x < 0, \\ u_R & \text{if } x > 0. \end{cases} \tag{2.3}$$

Recall that the characteristic speed of Eq. (1.1) is $f'(u)$. Thus, the characteristic speeds for Eq. (1.1) are either $1, 0$ or b, depending on whether $u < 0, 0 < u < 1$ or $u > 1$, respectively. Within each interval $(-\infty, 0), (0, 1)$, or $(1, \infty)$, the solution can jump, with the discontinuity propagating at the characteristic speed of that interval. These are linear discontinuities, which we consider to be admissible for all values of γ. It would be interesting to examine solutions of the corresponding linear equation with dissipation and dispersion, to establish the approximation of linear discontinuities by solutions of (1.2). We do not pursue this here.

Since the characteristic speed is piecewise constant, there are no centered rarefaction waves through which the solution varies continuously and the characteristics spread out in a fan. Within each interval $(-\infty, 0), (0, 1)$, or $(1, \infty)$, the rarefaction waves have been replaced by linear discontinuities. There are, however, pairs of discontinuities that, together, resemble a rarefaction wave. For example, if $u_L \in (0, 1)$ and $u_R \in (1, \infty)$, then there is a solution of the Riemann problem that has two discontinuities:

$$u(x,t) = \begin{cases} u_L & \text{if } x < 0, \\ 1 & \text{if } 0 < x < bt, \\ u_R & \text{if } x > bt. \end{cases} \tag{2.4}$$

Note that in the sector $0 < x < bt$, where $u = 1$, the characteristic speed is undefined. However, if we were to smooth the flux $f(u)$ near $u = 1$, so that $f'(u)$ runs smoothly and monotonically from zero to b as u travels from u_L to u_R, then the sector would be filled with characteristics and the solution would be a classical rarefaction wave. Because of this approximation, we regard these double linear discontinuities in (1.1) as admissible weak solutions of the Riemann problem.

A *centered shock wave*

$$u(x,t) = \begin{cases} u_- & \text{if } x < st, \\ u_+ & \text{if } x > st, \end{cases} \tag{2.5}$$

with speed s is a weak solution of (1.2) if the triple (u_-, u_+, s) satisfies the Rankine-Hugoniot condition

$$-s(u_+ - u_-) + f(u_+) - f(u_-) = 0. \tag{2.6}$$

Thus the shock speed

$$s = (f(u_+) - f(u_-))/(u_+ - u_-) \tag{2.7}$$

is the slope of the chord joining the points $(u_\pm, f(u_\pm))$ in the graph of f.

A shock (2.5) is called *compressive*, or a *Lax shock* if it satisfies the Lax entropy condition [7], which relates the slope of the chord, given by (2.7), to slopes of f:

$$f'(u_+) < s < f'(u_-). \tag{2.8}$$

Thus, every shock with $u_- \in (-\infty, 0) \cup (1, \infty)$ and $u_+ \in (0, 1)$ is a Lax shock.

To describe additional Lax shocks, it is convenient to define

$$u_b = b/(b-1). \tag{2.9}$$

Then there are Lax shocks from $u_- \in (-\infty, u_b]$ to $u_+ \in (1, \infty)$ (if $b < 1$), or from $u_- \in [u_b, \infty)$ to $u_+ \in (-\infty, 0)$ (if $b > 1$). The threshold of u_b for u_- is obtained from imposing the entropy condition (2.8), which requires the chord from u_- to u_+ to lie below or above the graph of f, respectively. Note that for $u_- = u_b$, we have $s = f'(u_+)$, so that such a shock is a generalized Lax shock in the sense that it is the limit of Lax shocks, and one of the inequalities (2.8) is replaced by an equality. Such a shock is related to the shock-rarefaction construction for nonconvex smooth flux functions, where here the rarefaction portion has degenerated into a line wave.

Additional shocks that extend the notion of Lax shock will be referred to as *special shocks*; they have $u_- < 0$ and $u_+ = 1$, or $u_- > 1, u_+ = 0$.

3. Traveling waves and undercompressive shocks. To describe γ-admissible shock waves, we consider traveling wave solutions $u = u(\xi)$, $\xi = (x - st)/\epsilon$ of (1.2) with the boundary conditions

$$u(\pm\infty) = u_\pm, \qquad u'(\pm\infty) = 0 = u''(\pm\infty). \tag{3.1}$$

Substituting into Eq. (1.2) and integrating from $\xi = -\infty$, we obtain the ordinary differential equation

$$\gamma u'' = -u' + f(u) - f(u_-) - s(u - u_-). \tag{3.2}$$

This second-order equation is equivalent to the first-order system

$$\begin{aligned} u' &= v, \\ \gamma v' &= -v + f(u) - f(u_-) - s(u - u_-). \end{aligned} \tag{3.3}$$

Equilibria of (3.3) are of the form (u, v), with $v = 0$, and

$$f(u) - f(u_-) - s(u - u_-) = 0. \tag{3.4}$$

If $(u_+, 0)$ is an equilibrium, then the Rankine-Hugoniot condition (2.6) holds, so that the triple (u_-, u_+, s) represents a shock wave solution (2.5) of the hyperbolic equation (1.1).

Now consider a chord through $(u_-, 0)$ with slope s such that the chord intersects the graph of f at two other values of u. The three intersections then correspond to equilibria for (3.3). If $\gamma > 0$, then the outside equilibria are saddle points, and the middle equilibrium is either a stable node if $4s\gamma < 1$, or a stable spiral if $4s\gamma > 1$.

As in the case of other nonconvex flux functions, there are γ-admissible shocks that are not Lax shocks, while some Lax shocks are not γ-admissible. The determination of which shocks are γ-admissible is made by studying the undercompressive shocks and their corresponding traveling waves.

If u_- and u_+ are saddle point equilibria for (3.3), and there is a heteroclinic orbit from $(u_-, 0)$ to $(u_+, 0)$ in the phase plane, then we say $u_- \to u_+$ is a *saddle-to-saddle connection.* Henceforth, we shall reserve the term *undercompressive shock* for a shock wave (2.5) that satisfies the Rankine-Hugoniot condition (2.6) and for which $u_- \to u_+$ is a saddle-to-saddle connection.

Let $u_- < 0$. We restrict attention to the range of s for which $(u_-, 0)$ is the left-most saddle point: $s < \min(1, b)$. At least near $(u_-, 0)$, the unstable manifold is a curve in the phase plane that can be parameterized by u. Let $v = v(u)$ along the unstable manifold through $(u_-, 0)$. We have the following relation:

$$\gamma \frac{1}{2}(v(u))^2 = \int_{u_-}^{u} v(y)\, dy - \int_{u_-}^{u} (f(y) - f(u_-) - s(y - u_-))\, dy. \tag{3.5}$$

In particular, if (u_-, u_+, s) corresponds to an undercompressive shock, then it is straightforward to check that the trajectory joining $(u_-, 0)$ to $(u_+, 0)$ is the graph of v over the interval $[u_-, u_+]$, and since $v(u) > 0$ for $u_- < u < u_+$, we have from $v(u_+) = 0$ and (3.5) that

$$\int_{u_-}^{u_+} (f(y) - f(u_-) - s(y - u_-))\, dy > 0, \tag{3.6}$$

that is, if $u_- \to u_+$ is a saddle-to-saddle connection, then the signed area between the graph of f and the chord with slope s intersecting the graph at $u = u_\pm$ must be *positive*.

Let $s = s_E(u_-, b)$ be the unique value of s for which the signed area is zero:

$$\begin{aligned} \int_{u_-}^{u_E} f(y)\, dy &= (f(u_E) + f(u_-))(u_E - u_-); \\ s_E(u_-, b) &= (f(u_E) - f(u_-))/(u_E - u_-) \\ &= 1 - ((u_- - 1)^2 - u_-^2/b)^{-1}. \end{aligned} \tag{3.7}$$

Equation (3.6) then implies that the range of values of s for which a saddle-to-saddle connection from u_- to some u_+ exists is restricted by

$$s < s_E(u_-, b). \tag{3.8}$$

When $b > 1$, there is no restriction on $u_- < 0$, but for $b < 1$, we must have

$$u_b < u_- < 0 \tag{3.9}$$

(u_b is given by (2.9)) in order to get a saddle-to-saddle connection. There is also a lower bound on s given by considering the chord in the graph of f that passes through the point (u_-, u_-) and the corner at $(1, 0)$:

$$s > \tilde{s}(u_-) \equiv \frac{u_-}{u_- - 1}. \tag{3.10}$$

To summarize, in order to have an undercompressive shock, we have thus far restricted the parameters u_-, s, b as follows:

$$\tilde{s}(u_-) < s < \min(s_E(u_-, b), b). \tag{3.11}$$

Note that for $b \geq 1$, we have $s_E(u_-, b) \leq 1$ and $\tilde{s}(u_-) < s_E(u_-, b)$ for all $u_- < 0$, whereas for $b < 1$, we have $\tilde{s}(u_-) < s_E(u_-, b)$ for all $u_- \in (u_b, 0)$. These restrictions are illustrated in Figures 4a and 4b.

a. *Integration of the ODE.* While inequalities (3.11) are necessary for an undercompressive shock with speed s, we only expect undercompressive shocks for isolated values of s, for each fixed u_-, γ, b. Finding these undercompressive shocks analytically for a general nonconvex flux f is not feasible. But for the trilinear flux of this paper, the ordinary differential equation (3.2) is piecewise linear. This simplification allows us to carry the analysis of undercompressive shocks quite far by integrating the ordinary differential equation directly. This is the approach of the present subsection.

Suppose there is a trajectory from $u_- < 0$ to $u_+ > 1$. Then the shock speed is given by the Rankine-Hugoniot condition (2.6):

$$s = (b(u_+ - 1) - u_-)/(u_+ - u_-). \tag{3.12}$$

To characterize the traveling wave, and parameter values for which the traveling wave exists, we consider solving the ordinary differential equation successively in the three domains for $u = u(\xi)$ in which $f(u)$ is affine (listed in the order in which they are treated):

$$\begin{aligned} &\textbf{LEFT:} && u_- \le u \le 0, \quad \xi \le 0; \\ &\textbf{RIGHT:} && 1 \le u \le u_+, \quad \xi \ge \xi_1; \\ &\textbf{MIDDLE:} && 0 \le u \le 1, \quad 0 \le \xi \le \xi_1. \end{aligned}$$

Here, we have fixed the phase in the solution by insisting on $u(0) = 0$, but there is an additional parameter ξ_1 that must be determined.

The ordinary differential equation (3.2) is

$$\gamma u'' + u' = f(u) - su + C, \tag{3.13}$$

where $C = (s-1)u_-$ is the same constant in all three domains.

LEFT: (3.13) becomes

$$\gamma u'' + u' + (s-1)u = (s-1)u_-, \tag{3.14}$$

with boundary conditions

$$u(-\infty) = u_-; \qquad u(0) = 0. \tag{3.15}$$

The solution we seek follows the unstable manifold from the equilibrium $(u_-, 0)$ with increasing u:

$$u(\xi) = u_-(1 - e^{r\xi}), \quad \xi < 0, \quad r = \frac{1}{2\gamma}\left(-1 + \sqrt{1 + 4\gamma(1-s)}\right). \tag{3.16}$$

RIGHT: (3.13) becomes

$$\gamma u'' + u' + (s-b)u = (s-b)u_+, \tag{3.17}$$

with boundary conditions

$$u(\xi_1) = 1; \qquad u(\infty) = u_+. \tag{3.18}$$

The solution follows the stable manifold of $(u_+, 0)$, toward decreasing u:

$$u(\xi) = u_+ + (1 - u_+)e^{p(\xi - \xi_1)}, \quad \xi > \xi_1, \quad p = \frac{1}{2\gamma}\left(-1 - \sqrt{1 + 4\gamma(b-s)}\right). \tag{3.19}$$

MIDDLE: (3.13) becomes

$$\gamma u'' + u' + su = (s-1)u_-, \tag{3.20}$$

with boundary conditions

$$u(0) = 0: \qquad u(\xi_1) = 1. \tag{3.21}$$

The solution of (3.20) is of the form

$$u(\xi) = \alpha e^{q_+\xi} + \beta e^{q_-\xi} + \frac{s-1}{s}u_-, \quad 0 < \xi < \xi_1, \quad q_\pm = \frac{1}{2\gamma}(-1 \pm \sqrt{1-4\gamma s}). \tag{3.22}$$

It remains to choose α, β, ξ_1 and s so that u and u' are continuous at both $\xi = 0$ and $\xi = \xi_1$. Continuity at ξ_1 leads directly to the equations

$$\begin{aligned} \alpha e^{q_+\xi_1} + \beta e^{q_-\xi_1} + \frac{s-1}{s}u_- &= 1, \\ \alpha q_+ e^{q_+\xi_1} + \beta q_- e^{q_-\xi_1} &= (1-u_+)p, \end{aligned} \tag{3.23}$$

in which the coefficients α, β are found by imposing continuity at $\xi = 0$:

$$\begin{aligned} \alpha &= \frac{u_-}{q_+ - q_-}((s-1)q_- - sr), \\ \beta &= -\frac{u_-}{q_+ - q_-}((s-1)q_+ - sr). \end{aligned} \tag{3.24}$$

Additionally, we have the Rankine-Hugoniot relation between u_-, u_+ and s, written as

$$1 - u_+ = \frac{s}{s-b}\left(1 - \frac{s-1}{s}u_-\right).$$

Thus we can equate exponentials in (3.23), leading to an equation for ξ_1:

$$e^{(q_+-q_-)\xi_1} = \frac{((s-1)q_+ - sr)((s-b)q_- - sp)}{((s-1)q_- - sr)((s-b)q_+ - sp)}. \tag{3.25}$$

Applying the definitions of the constants $q_\pm, p, r$, we obtain

$$e^{(q_+-q_-)\xi_1} = \frac{(1+(s-1)R_0 - sR_1)(b-(s-b)R_0 + sR_b)}{(1-(s-1)R_0 - sR_1)(b+(s-b)R_0 + sR_b)}, \tag{3.26}$$

in which

$$R_\theta = \sqrt{1 - 4\gamma s + 4\gamma\theta}, \quad \theta = 0, 1, b.$$

b. *Nonexistence of undercompressive shocks for small γ.*

THEOREM 3.1. Let $u_- < 0$, $u_+ > 1$, with corresponding shock speed $s < \min(1, b)$. If $4\gamma s < 1$, then there is no traveling wave from u_- to u_+.

Proof. The proof is based upon showing that the right-hand side of (3.26) is less than unity. Since $q_+ - q_- > 0$, this would imply $\xi_1 < 0$, which is inconsistent with the construction of the solution.

First note that R_0, R_1, R_b are all real for $4\gamma s < 1$, and so are $q_\pm$. We have

$$q_+ - q_- = \frac{1}{\gamma}\sqrt{1-4\gamma s} > 0; \quad R_0 < 1; \quad 1 < R_1 < R_b \text{ if } b > 1; \quad 1 < R_b < R_1 \text{ if } b < 1. \tag{3.27}$$

LEMMA 3.2. $sR_1 < 1$ for $0 < s < \min(1, \frac{1}{4\gamma})$.

Proof. Let

$$g(s) = (sR_1)^2 - 1 = (1 + 4\gamma)s^2 - 4\gamma s^3 - 1.$$

Then g has one negative zero and two positive roots, including $s = 1$.

First consider $\gamma \leq \frac{1}{4}$. Then $g'(1) = 2 - 4\gamma > 0$. Since $g(0) < 0$, this implies that $s = 1$ is the smaller of the two positive zeroes of g, so that $g(s) < 0$ for all s, $0 < s < 1$.

For $\gamma > \frac{1}{4}$, we have to show $g(s) < 0$ for $0 < s < \frac{1}{4\gamma} < 1$. But the only local maximum of $g(s)$ occurs at $s = \frac{2}{3} + \frac{1}{6\gamma} > \frac{1}{4\gamma}$ (for $\gamma > \frac{1}{4}$), and $g(\frac{1}{4\gamma}) < 0$. Since $g(0) < 0$, this completes the proof of the lemma. □

To complete the proof of the theorem, we first prove the result for $b = 1$, then for $b < 1$, by comparison with $b = 1$, and finally we prove the result for $b > 1$. Let Q_b denote the right-hand side of Eq. (3.26).

(i) $b = 1$. We express the right-hand side of (3.26) as

$$Q_1 = \frac{(1 - U - V)(1 + U + V)}{(1 + U - V)(1 - U + V)}, \tag{3.28}$$

where

$$U = (1 - s)R_0; \qquad V = sR_1$$

are both positive. Thus,

$$Q_1 = \frac{1 - (U + V)^2}{1 - (U - V)^2} < 1,$$

provided $1 - (U - V)^2 > 0$. But

$$\begin{aligned} 1 - (U - V)^2 &= (1 + U - V)(1 - U + V) \\ &= (1 + (1 - s)R_0 - sR_1)(1 - R_0 + s(R_0 + R_1)) > 0, \end{aligned}$$

by (3.27) and Lemma 3.2. This completes the proof of the theorem in the case $b = 1$.

(ii) $b < 1$. By part (i), to show $Q_b < 1$, it is enough to prove $Q_b < Q_1$, which reduces to

$$F(b) \leq F(1), \tag{3.29}$$

where

$$F(b) \equiv \frac{b + sR_b + (b - s)R_0}{(b + sR_b - (b - s)R_0)} \quad \text{for } s < b < 1.$$

Now $F(b) = \frac{1+G(b)}{1-G(b)}$, where $G(b) = \frac{(b-s)R_0}{b+sR_b}$. Note that showing $0 < G(b) < 1$ and $G(b) \leq G(1)$ would imply (3.29). The latter inequality reduces to

$$(1 + sR_1)(b - s)R_0 \leq (1 - s)R_0(b + sR_b),$$

i.e., we need to show

$$(1 - s)R_b \geq (b - s)R_1 - 1 + b. \tag{3.30}$$

Rearranging and substituting the definition of R_b, this becomes

$$(1 - s)\sqrt{1 + 4\gamma b - 4\gamma s} \geq b(1 + R_1) - (1 + sR_1). \tag{3.31}$$

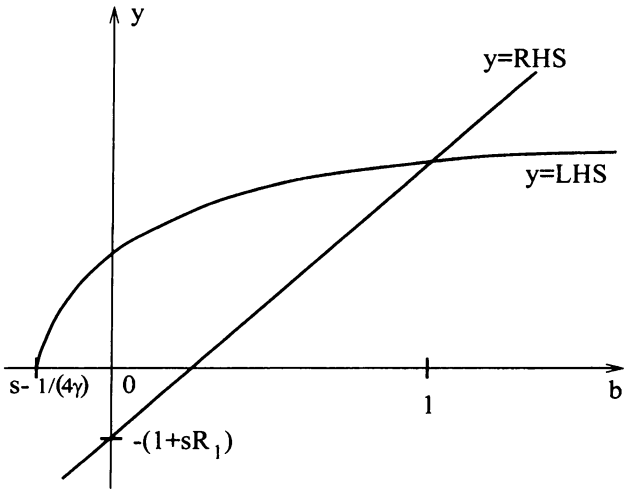

FIG. 2. Left and right sides of inequality (3.31)

The left-hand side of this inequality is a square-root function of b, whereas the right-hand side is linear in b. The graphs are sketched in Fig. 2. In particular, the left-hand side and right-hand side are equal at $b = 1$; the left-hand side is positive for $b \geq 0$, and the right-hand side is negative at $b = 0$. These observations are enough to verify the inequality (3.31), which confirms (3.29), and hence completes the proof for $b < 1$.

(iii) $b > 1$. The proof in this case follows a similar pattern. First, we observe from Lemma 3.2 that $sR_b < b$ for $s < 1, b > 1$. This follows from

$$\frac{s}{b}R_b = \frac{s}{b}\sqrt{1 - 4\gamma s + 4\gamma b} = t\sqrt{1 - 4\gamma' t + 4\gamma'},$$

where $t = s/b < 1$; $\gamma' = \gamma b$. Correspondingly, we can transform Q_1 from part (i) into

$$\overline{Q}_b = \frac{(1 + (t-1)R_0 - tR_b)(1 + tR_b + (1-t)R_0)}{(1 - (t-1)R_0 - tR_1)(1 + tR_b - (1-t)R_0)}, \tag{3.32}$$

where $t = s/b$. Thus, $\overline{Q}_b < 1$ for $t < \min(1, \frac{1}{4b\gamma})$. Comparing (3.26) with (3.32), we see that to prove $Q_b \leq \overline{Q}_b < 1$, we need only show

$$\frac{(1 + (s-1)R_0 - sR_1)}{(1 - (s-1)R_0 - sR_1)} \leq \frac{(1 + (t-1)R_0 - tR_b)}{(1 + tR_b - (1-t)R_0)} \tag{3.33}$$

for $b > 1$, $t = s/b$. As in part (ii), we reduce this inequality to showing

$$(1 - s)R_b \leq (b - s)R_1 - 1 + b. \tag{3.34}$$

However, checking (3.34) is subtler than for (3.30) because both the left- and right-hand sides are positive at $b = 0$. However, the inequality does hold at $b = 0$. Therefore, it is enough to show that the derivative of the difference (left- minus right-hand sides) is negative at $b = 1$. We leave the details to the reader. This completes the proof of the theorem. □

Together with the restriction $s < \min(1, b)$, the theorem leads to the following conclusion.

COROLLARY 3.3. For $\gamma < \frac{1}{4}\max(1, \frac{1}{b})$, there are no γ-admissible undercompressive shocks.

This result is in striking contrast with the situation for a scalar equation with cubic flux function, where even a small amount of dispersion (i.e., γ arbitrarily small) is enough to generate undercompressive shocks [6]. However, a threshold similar to that in the corollary is encountered for the p-system with a monotonic cubic flux [9].

c. *Existence of undercompressive shocks for sufficiently large* γ. The restriction $4\gamma s > 1$ on undercompressive shocks is shown in Fig. 4. In that figure, we have also represented inequalities (3.11). We now show that these are the only restrictions on the parameters in the sense of the following theorem. For $\gamma > \frac{1}{4}$, let $u_{\max}(\gamma) = -1/(4\gamma - 1)$ be the value of u_- at the intersection of the curves $s = \tilde{s}(u_-)$ and $s = \frac{1}{4\gamma}$ (see Fig. 4), and for $b < 1$, let $u_{\min}(b) = b/(b-1)$ be the value of u_- at which $s = \tilde{s}(u_-) = b$. (Note that $u_{\min}(b) = u_b$ for $b < 1$.) For $b > 1$, let $u_{\min} = -\infty$. Note that, as indicated in Fig. 4, $u_{\min}(b) < u_{\max}(\gamma)$ for $\gamma > \frac{1}{4}\max(1, \frac{1}{b})$. For each $u_- \in (u_{\min}(b), u_{\max}(\gamma))$, and each $s \in (\tilde{s}(u_-), s_E(u_-, b))$, let $u_+ > 1$ be given by the Rankine-Hugoniot condition (2.6), i.e., $u_+ = (b + (1-s)u_-)/(b-s)$.

THEOREM 3.4. Let $\gamma > \frac{1}{4}\max(1, \frac{1}{b})$. Then for each $u_- \in (u_{\min}(b), u_{\max}(\gamma))$, there is a unique $s = s_\Sigma(u_-; \gamma, b) \in (\tilde{s}(u_-), s_E(u_-, b))$ such that the shock wave (2.5) is a γ-admissible undercompressive shock.

Proof. To prove existence of a trajectory from $(u_-, 0)$ to $(u_+, 0)$ for some value of s in the interval of the theorem, we use a simple argument based on the separation between the unstable manifold of $(u_-, 0)$ and the stable manifold of $(u_+, 0)$.

The argument depends partly on the structure of the explicit solution calculated earlier. Specifically, when $s = \tilde{s}(u_-)$, then $u_+ = u_m = 1$. Since $4\gamma s > 1$, R_0 is imaginary: $R_0 = i\omega$, where $\omega = \sqrt{4\gamma s - 1}$, and $q_\pm = \frac{1}{2\gamma}(-1 \pm i\omega)$ are complex. However, R_1, R_b, p and r remain real, since $s < \min(1, b)$. Now for $\xi > 0$, the calculation of the trajectory in the middle section $0 \le u < 1$ gives

$$u(\xi) = \frac{u_-}{s\omega} e^{-\xi/(2\gamma)}((1-s)\omega\cos\theta + (1 - R_1 s)\sin\theta) + \frac{s-1}{s}u_-, \tag{3.35}$$

where $\theta = \omega\xi/(2\gamma)$. Note that $u(0) = 0$, and that (from the construction of $u(\xi)$) $u'(0) > 0$.

In particular, for $s = \tilde{s}(u_-)$, we have $\frac{s-1}{s}u_- = u_+ = 1$, so that $\lim_{\xi\to\infty} u(\xi) = 1$. Moreover, from (3.35), u oscillates about $u = 1$; so there exists a first $\xi = \xi_1 > 0$ such that $u(\xi_1) = 1$, for which necessarily $u'(\xi_1) > 0$. Thus, in the (u, u') phase plane, $(u(\xi_1), u'(\xi_1))$ lies above $(u_+, 0) = (1, 0)$, so that the entire unstable manifold from $(u_-, 0)$ lies above the stable manifold emanating from $(u_+, 0)$.

On the other hand, for $s = s_E(u_-, b)$, the unstable manifold from $(u_-, 0)$ must cross the u-axis to the left of $u = u_+$, by (3.5), and so must lie under the stable manifold emanating from $(u_+, 0)$. Thus, there is a value of s in the interval $(\tilde{s}(u_-), s_E(u_-, b))$ for which the two manifolds coincide, giving a saddle-to-saddle connection corresponding to an undercompressive shock. Uniqueness follows as in [4] by showing that the derivative

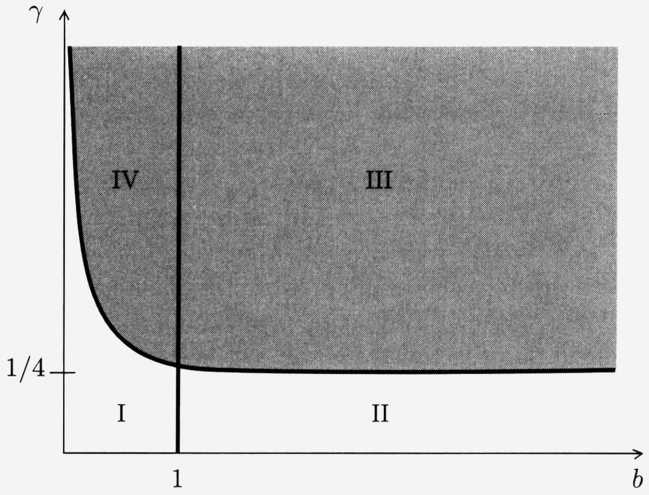

FIG. 3. Undercompressive shocks occur only for (b, γ) in the shaded areas

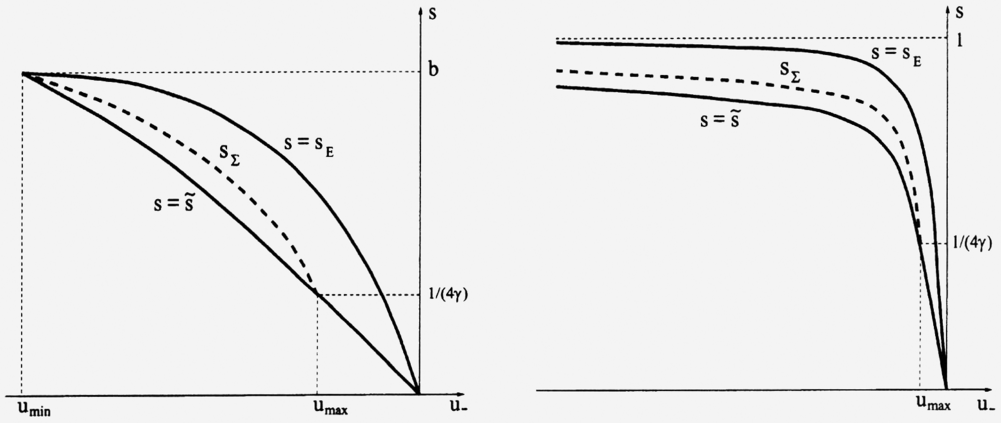

4a. $\frac{1}{4\gamma} < b < 1$ 4b. $\frac{1}{4\gamma} < 1 < b$

FIG. 4. Undercompressive shock speed $s_\Sigma(u_-; b, \gamma)$

with respect to s of the separation between these manifolds is nonzero when there is a saddle-to-saddle connection. This completes the proof of Theorem 3.4. □

Restrictions on γ, b for the existence of undercompressive shocks are shown in Fig. 3. In Fig. 4, we show the dependence of $s_\Sigma(u_-; b, \gamma)$ on u_- for typical values of γ, b. Numerical calculations are shown in Fig. 5, indicating the dependence on γ.

d. *Admissible shocks.* One consequence of the presence of γ-admissible undercompressive shock waves is that some Lax shocks are not γ-admissible. This is a routine observation (cf. [4, 6]); so we simply summarize the result in the present context.

Consider a Lax shock

$$u_{\text{Lax}}(x,t) = \begin{cases} u_- & \text{if } x < st, \\ u_+ & \text{if } x > st, \end{cases} \tag{3.36}$$

in which $u_- < 0$, $0 < u_+ < 1$. Suppose that there is a γ-admissible undercompressive shock

$$u_\Sigma(x,t) = \begin{cases} u_- & \text{if } x < s_\Sigma t, \\ \overline{u} & \text{if } x > s_\Sigma t, \end{cases} \tag{3.37}$$

with $\overline{u} > 1$. Let

$$u_m = u_m(u_-) = (1 - s_\Sigma^{-1})u_- \in (0,1) \tag{3.38}$$

denote the middle equilibrium for the vector field (3.3). Then u_{Lax} is γ-admissible if and only if

$$u_+ < u_m.$$

If there is no undercompressive shock with $u_- < 0$ on the left, then u_{Lax} is γ-admissible for all $u_+ \in (0,1)$.

The following observation follows easily from the area rule (3.6). With respect to the same undercompressive shock u_Σ of (3.37), note that

$$u(x,t) = \begin{cases} \overline{u} & \text{if } x < st, \\ u_+ & \text{if } x > st \end{cases} \tag{3.39}$$

(with $s(u_+ - \overline{u}) = f(u_+) - f(\overline{u})$) is a γ-admissible Lax shock for $u_m < u_+ < 1$, which implies $s_\Sigma < s < b$.

Here is a summary of the elementary discontinuous waves

$$u(x,t) = \begin{cases} u_- & \text{if } x < st, \\ u_+ & \text{if } x > st, \end{cases} \tag{3.40}$$

considered admissible, to be used in the next section:

Linear waves $\mathcal{L}_1; \mathcal{L}_0; \mathcal{L}_b$: These solutions have either $u_-, u_+ < 0$, $s = 1$; $0 < u_-, u_+ < 1$, $s = 0$; or $1 < u_-, u_+$, $s = b$, respectively.

γ-admissible Lax shocks S: These are of the form (3.40) with u_-, u_+ in various ranges. For example, $u_- < 0$, $0 < u_+ < u_m(u_-)$ if there is an undercompressive shock (3.37), and $0 < u_+ < 1$ if not. We also denote by S the γ-admissible Lax shocks (3.39). γ-admissible Lax shocks also occur when $b < 1$, $u_- < u_b$ and $u_+ > 1$.

Undercompressive shocks Σ: These are controlled by Theorem 3.1, Corollary 3.3, and Theorem 3.4.

Special shocks $\widetilde{\mathbf{S}}$: In these solutions, $u_- < 0$ and $u_+ = 1$, $s = \tilde{s} = u_-/(u_- - 1)$, provided there is no undercompressive shock (3.37). Note that if $b < 1$, and $u_- < u_b = b/(b-1)$, then $\widetilde{S}$ corresponds to a single point embedded in a one-parameter family of S shocks. In this case, we do not separately label $\widetilde{S}$, but simply regard it as an S shock.

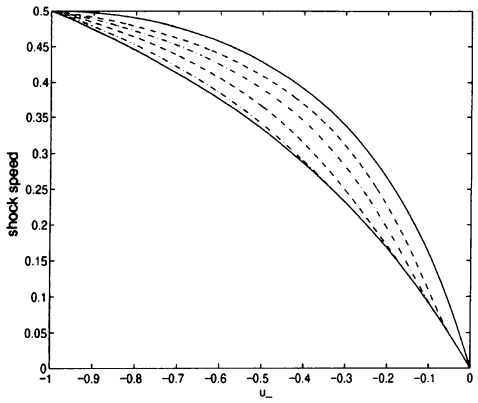

5a. $b = 0.5$

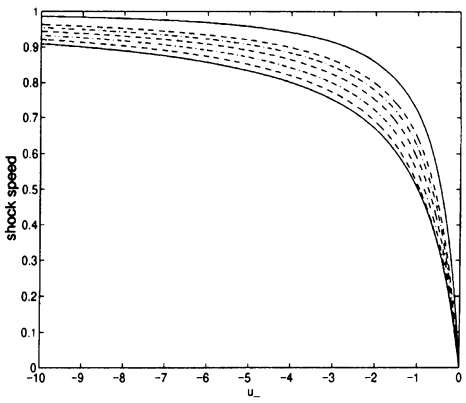

5b. $b = 2$

FIG. 5. Numerical values of $s_\Sigma(u_-; b, \gamma)$ for $\gamma = 1, 2, 4, 8, 16$

c. *Solution of the algebraic equations for the traveling wave.* We now describe the explicit solution of equations (3.23) characterizing γ-admissible undercompressive shocks, for (b, γ) in the shaded region of Fig. 3. Since $4\gamma s > 1$, we set

$$q_\pm = -1/(2\gamma) \pm i\omega, \quad \text{where } \omega = \sqrt{4\gamma s - 1}.$$

Equations (3.23) then become

$$\begin{aligned} \mathrm{Re}(\alpha e^{q+\xi_1}) &= (1 - u_m)/2, \\ \mathrm{Re}(\alpha q_+ e^{q+\xi_1}) &= p(1 - u_+)/2, \end{aligned} \tag{3.41}$$

in which (3.24) gives

$$\alpha = -u_m/2 + i\phi, \quad \text{where } \phi = \frac{ru_-}{2\omega} + \frac{u_m}{4\gamma\omega}. \tag{3.42}$$

Note that both right sides of equations (3.41) are positive. For a fixed choice of u_-, we solve (3.41) for ξ_1 and s in two stages. Initially, we isolate ξ_1, which is now a function of s, as follows: from (3.42) we have

$$e^{q+\xi_1} = e^{-\xi_1/(2\gamma)}(\cos\omega\xi_1 + i\sin\omega\xi_1),$$

so that solving for $e^{q+\xi_1}$ in (3.41), we obtain

$$\tan\omega\xi_1 = \psi, \quad \text{where } \psi \equiv \frac{2\omega\phi(1 - u_m) - \chi u_m}{\omega u_m(1 - u_m) + 2\phi\chi},$$

and $\chi \equiv p(1 - u_+) + (1 - u_m)/(2\gamma)$. Thus,

$$\xi_1 = \frac{1}{\omega}\tan^{-1}\psi + j\pi, \tag{3.43}$$

with $j = 0, 1$ or 2.

Equipped with formula (3.43) for $\xi_1(s)$, we now use interval subdivision to find s, and hence ξ_1. From Theorem 3.4, we have that for a given $u_- \in (u_{\min}, u_{\max})$, the shock speed is restricted to the interval $s \in (\tilde{s}(u_-), s_E(u_-))$. Starting at the ends of this shock-speed

interval, we compute $\xi_1(s)$ via (3.43), with j chosen such that (i) $\xi_1 > 0$ and (ii) the left sides of (3.41) are positive. We then find the difference of the left and right sides of both equations (3.41). The shock-speed interval is then halved repeatedly, until we find the value, $s_\Sigma(u_-; b, \gamma)$, at which the differences of both left and right sides of (3.41) change signs. While one equation of (3.41) would be sufficient to solve for s and $\xi(s)$, we used both equations as a check. The numerical solutions obtained in this manner are shown in Figures 5a and 5b, for fixed, representative choices of $b < 1$ and $b > 1$, respectively. The nested, dashed curves correspond to several choices of γ for each value of b.

4. The Riemann problem. The Riemann problem is the initial value problem

$$u_t + f(u)_x = 0,$$
$$u(x,0) = \begin{cases} u_L & \text{if } x < 0, \\ u_R & \text{if } x > 0. \end{cases} \tag{4.1}$$

We construct centered solutions (i.e., functions of x/t) that are combinations of linear discontinuities and γ-admissible shocks. The solution depends on four parameters. The parameters $b > 0$ and $\gamma > 0$ define the equation, and provide the admissibility condition for shocks; the parameters u_L, u_R constitute initial data for the solution of a specific equation (fixed b) with a given admissibility criterion (fixed γ) for nonlinear discontinuities.

In Fig. 3, we show the (b, γ)-plane, divided into four regions. The regions correspond to the restrictions of Corollary 3.3 and Theorem 3.4. Specifically, for $b < 1$, there can be undercompressive shocks in the Riemann problem only for $\gamma > 1/(4b)$, whereas for $b > 1$, there can be undercompressive shocks only for $\gamma > 1/4$. In particular, the shaded region corresponds to values of b, γ for which the solution of the Riemann problem has an undercompressive shock for some choices of the data u_L, u_R, making it nonclassical in the sense of [2].

In Figures 6a, 6b, 7a, and 7b, we represent in the (u_L, u_R)-plane the various combinations of elementary waves in the solution of the Riemann problem.

REMARK 1. Because of the symmetry $b \to 1/b, u_L \to 1 - u_L$ in the Riemann problem, we may restrict attention to $u_L < 1/2$, allowing all positive values of b.

REMARK 2. The regions in the (u_L, u_R)-plane in which either $0 < u_L < 1/2$ or $u_R < 0$ are shown only in Fig. 6a, since they retain the same combinations of waves in the other cases. Omitting these regions from Figures 6b, 7a, and 7b helps keep those figures relatively simple and focused on the interesting features of the solution.

In what follows, we describe case-by-case the various regions in the (u_L, u_R)-plane and the transitions between combinations of waves.

Case I, *Figure* 6a: $b < 1$ *and* $\gamma < 1/(4b)$. First consider $0 < u_L < 1/2$. If $0 < u_R < 1$, the solution of the Riemann problem is independent of time:

$$u(x,t) = \begin{cases} u_L & \text{if } x < 0, \\ u_R & \text{if } x > 0. \end{cases} \tag{4.2}$$

If $u_R < 0$, then the solution has a double linear wave structure:

$$u(x,t) = \begin{cases} u_L & \text{if } x < 0, \\ 0 & \text{if } 0 < x < t, \\ u_R & \text{if } x > t. \end{cases} \tag{4.3}$$

Finally, and similarly, if $u_R > 1$, then the solution also has a double wave:

$$u(x,t) = \begin{cases} u_L & \text{if } x < 0, \\ 1 & \text{if } 0 < x < bt, \\ u_R & \text{if } x > bt. \end{cases} \tag{4.4}$$

Next, consider $u_L < 0$. Then if $u_R < 0$, the solution is a linear wave:

$$u(x,t) = \begin{cases} u_L & \text{if } x < t, \\ u_R & \text{if } x > t. \end{cases} \tag{4.5}$$

If $0 < u_R < 1$, the solution consists of a single, γ-admissible Lax shock, since undercompressive shocks are not allowed. When $u_R > 1$, however, there are two cases to consider. Since $b < 1$, a Lax shock from u_L to u_R is allowed, provide u_L is negative enough that the chord from u_L to u_R in the graph of f lies below the graph of f. The threshold value for this property is $u_L = u_b = b/(b-1)$. Thus, for $u_L < u_b$, the solution of the Riemann problem for $u_R > 0$ is a single Lax shock (4.5), whereas for $u_b < u_L < 0$, this solution is valid only for $0 < u_R < 1$; for $u_R > 1$, the solution consists of a pair of discontinuities: a special shock and a linear wave,

$$u(x,t) = \begin{cases} u_L & \text{if } x < \tilde{s}t, \\ 1 & \text{if } \tilde{s}t < x < bt, \\ u_R & \text{if } x > bt, \end{cases} \tag{4.6}$$

in which the speed $\tilde{s}$ is the slope of the chord from u_L to $u = 1$: i.e., $\tilde{s} = u_L/(u_L - 1)$, and the corresponding shock is indicated by the notation $\tilde{S}$ in Fig. 6.

Case II, *Figure* 6b: $b > 1$ *and* $\gamma < 1/4$. The transition from Fig. 6a to Fig. 6b is explained by the fact that as $b \to 1-$, $u_b \to -\infty$.

Case III, *Figure* 7a: $b > 1$ *and* $\gamma > 1/4$. Now for $u_L < u_{\max} = 1/(1-4\gamma)$, there is a range of u_R for which the solution of the Riemann problem is nonclassical due to the inclusion of an undercompressive shock.

For $u_{\max} < u_L < 0$, the solution is the same as for Cases I and II. For $u_L < u_{\max}$, the solution has a single Lax shock for $0 < u_R < u_m$. For $u_R > u_m$, the solution involves an undercompressive shock (denoted as Σ in Figures 7a, 7b) from u_L to $u_+(u_L)$, either combined with a Lax shock S, or combined with a linear discontinuity, $\mathcal{L}_b$, of speed b.

Values of (u_L, u_R) for which the solution of the Riemann problem is nonmonotonic lie in the shaded region of Fig. 7a and there is a similar shaded region in Fig. 7b. The upper boundary of this region is the curve Σ representing the pairs (u_L, u_R) for which there is an undercompressive shock from u_L to u_R.

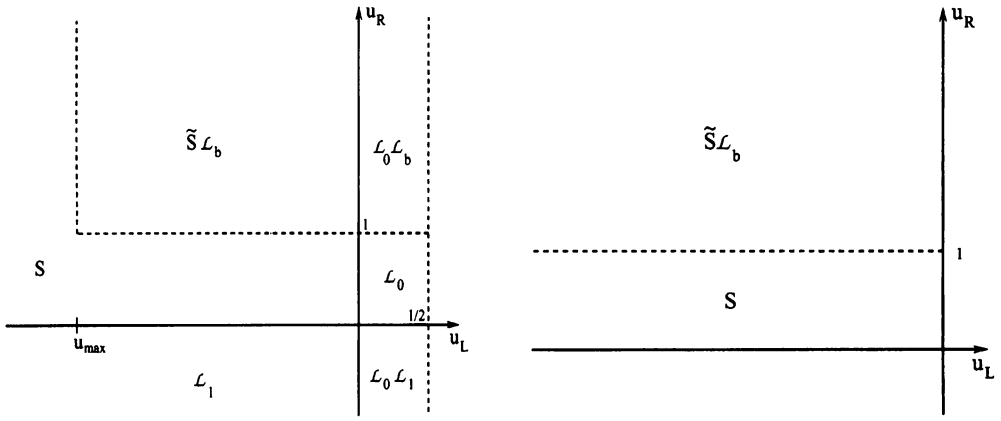

6a. Case I

6b. Case II

FIG. 6. Solution of the Riemann problem for (b, γ) in the first and second regions of Fig. 3

In Lemma 4.1 below, we show that as $u_L \to -\infty$, $u_m(u_L)$ approaches an asymptotic value $u_M(\gamma) > 0$. Correspondingly, the curve Σ approaches $(b - u_M(\gamma))/(b-1)$ asymptotically, as $u_L \to -\infty$.

a. *Case IV, Figure 7b: $b < 1$ and $\gamma > 1/(4b)$.* As in Case I, u_b is finite, and as $u_L \to u_b+$, the speed of the undercompressive shock from u_L to $u_+(u_L)$ approaches b, while $u_m(u_L)$ approaches $u = 1$ (as shown in Fig. 7b). For $u_L < u_b$, the only shocks from u_L to $u > 1$ are Lax shocks, so that the region of the (u_L, u_R)-plane that includes undercompressive shocks is cut off at $u_L = u_b$.

Note that since $u_m(u_{\max}) = 1 = u_m(u_b)$ and $u_m \not\equiv 1$, the curve $u_m(u_L)$ is nonmonotone. The curve drawn in Fig. 7b is typical of those we found in the numerical solution of the traveling wave equations. This nonmonotonicity of u_m is a departure from the cubic case [6], in which the corresponding u_m depends only on γ.

LEMMA 4.1. For each $b > 1$, the middle equilibrium $u_m(u_-)$ for an undercompressive shock with left state u_- has the following asymptotic behavior as $u_- \to -\infty$:

$$\lim_{u_- \to -\infty} u_m(u_-) > 0.$$

Proof. First note from (3.10) that $\lim_{u_- \to -\infty} \tilde{s}(u_-) = 1$ and $\lim_{u_- \to -\infty} s_E(u_-) = 1$, so that

$$\lim_{u_- \to -\infty} s_\Sigma(u_-) = 1. \tag{4.7}$$

Now $u_m(u_-) = \frac{(s-1)}{s} u_-$, where $s = s_\Sigma(u_-)$. Thus

$$\lim_{u_- \to -\infty} u_m(u_-) = \lim_{u_- \to -\infty} (s-1)u_-. \tag{4.8}$$

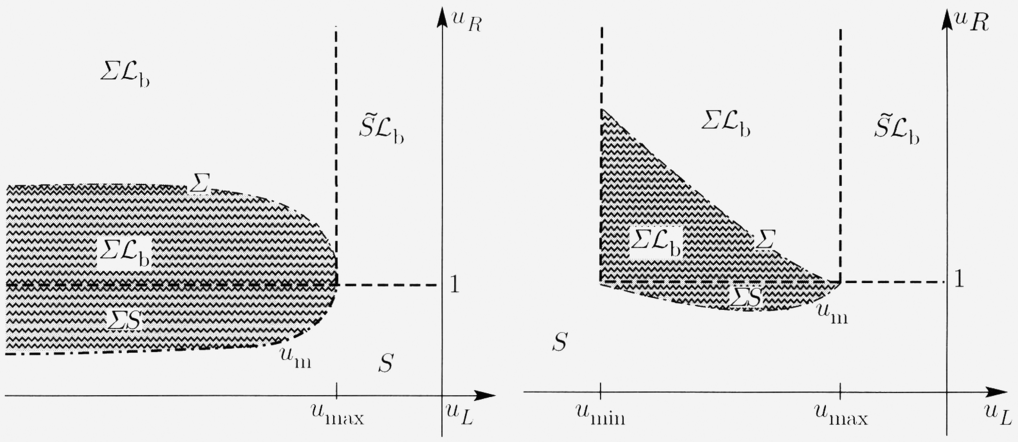

7a. Case III 7b. Case IV

FIG. 7. Solution of the Riemann problem for (b, γ) in the third and fourth regions of Fig. 3

Let $\xi_1(u_-)$ be the value of $\xi_1 > 0$ in (3.26), corresponding to an undercompressive shock. Using (4.7), we calculate from (3.26) that

$$\lim_{u_- \to -\infty} e^{(q_+ - q_-)\xi_1(u_-)} = \frac{(1 - 2\gamma - i\omega)(b + 1 + i(b-1)\omega)}{(1 - 2\gamma + i\omega)(b + 1 - i(b-1)\omega)},$$

where $\omega = \sqrt{4\gamma - 1}$. (In deriving the limit, we have used $R_0 = i\omega$, $R_b \to 1$, and $1 - sR_1 \sim (1 - s)(1 - 2\gamma)$.) In particular, the limit exists.

Now $\lim_{u_- \to -\infty} u_m(u_-)$ can in principle be computed from (3.23, 3.24). Instead of computing this formula, we follow the easier route of showing that the limit has to be positive for each $\gamma < \infty$. Suppose for a contradiction that

$$\lim_{u_- \to -\infty} u_m(u_-) = 0. \tag{4.9}$$

(Note that the limit has to be in the interval $[0, 1]$ since $0 < u_m(u_-) < 1$.) Now write the first equation of (3.23) in the form

$$2\,\mathrm{Re}(\alpha e^{q_+ \xi_1(u_-)}) + u_m(u_-) = 1. \tag{4.10}$$

But $q_+ = (-1 + i\omega)/(2\gamma)$, so that

$$|e^{q_+ \xi_1(u_-)}| < 1.$$

Moreover, from (3.24, 4.8),

$$\lim_{u_- \to -\infty} |\alpha / u_m(u_-)| < \infty,$$

so that $\alpha \to 0$ as $u_- \to -\infty$. Therefore, assuming (4.9), the left-hand side of (4.10) approaches zero as $u_- \to -\infty$, a contradiction. □

REMARK. In the purely dispersive case, corresponding to $\gamma \to \infty$, we have $s_\Sigma = s_E$. From the asymptotic behavior of s_E (given by (3.7)) as $u_- \to -\infty$:

$$s_E(u_-) \sim 1 - K/u_-^2,$$

we deduce that $u_m(u_-) = (1 - s_E(u_-)^{-1})u_- \sim 1/|u_-| \to 0$ as $u_- \to -\infty$. This suggests that the asymptote $u_{MI}(\gamma)$ of γ in Fig. 7a approaches zero as $\gamma \to \infty$.

5. Numerical results. The analysis of previous sections has focused on traveling wave solutions of the diffusive-dispersive equation (1.2). Moreover, in Subsection 3e, we presented numerical solutions of equations that determine parameter values for undercompressive shock waves. In this section, we consider numerical simulations of the partial differential equation (1.2) itself. Our purpose is to confirm the earlier results by displaying the structure of Riemann solutions containing undercompressive shocks, when small dissipation and dispersion are included.

The numerical scheme we employ was introduced in [3] and utilized in [4]. The novel feature of this scheme is that it takes a high-order discretization of the (piecewise linear) flux, so that the modified equation (including truncation error) agrees with the regularized PDE (1.2). The hope is that by mimicking the augmented equation, the undercompressive shocks computed by the scheme will accurately match those found via traveling-wave arguments—at least when the shock strength is not too large. Indeed, this is what was found in the case of the *cubic* nonlinear flux: numerical solutions showed excellent agreement with traveling wave solutions (cf. [3, 6]).

The scheme we use is continuous-in-time, discrete-in-space, and has the following form:

$$\frac{du_j}{dt} + \frac{g_{j+1/2} - g_{j-1/2}}{h} = \epsilon \frac{u_{j+1} - 2u_j + u_{j-1}}{h^2} + \gamma\epsilon^2 \frac{u_{j+2} - 2u_{j+1} + 2u_{j-1} - u_{j-2}}{2h^3}, \tag{5.1}$$

where $u_j = u_j(t)$ approximates $u(jh, t)$, with h being the mesh-spacing. The numerical flux $g_{j+1/2}(u)$ is given by

$$g_{j+1/2} = \tfrac{1}{12}(-f(u_{j+2}) + 7f(u_{j+1}) + 7f(u_j) - f(u_{j-1})), \tag{5.2}$$

where $f(u_j)$ is the trilinear flux (2.2), evaluated at $u = u_j$. The system of ordinary differential equations (5.1) was integrated using the fourth-order Runge-Kutta scheme. For further details about the numerical method, we refer the reader to [3].

In Fig. 8a, we plot the solution of (5.1) with Riemann initial data $u_L = -0.696$ and $u_R = 0.9$. This solution contains an undercompressive shock from u_L to a well-defined intermediate state $u_m = 1.2587$. To the right of this state is a Lax shock from u_m to u_R, containing some post-shock oscillations. In this figure, $h = 1/400$, $\gamma = 4$ and $b = 0.75$. For these values of u_L, b and γ, the analytical value of $u_+(u_L)$ is $u_+ = 1.2593$ (calculated as in Subsection 4e), making the numerical error in u_+ about 0.04%. The value $u_L = -0.696$ was chosen because it is very close to the minimum of $u_m(u_L)$ (cf. Fig. 5d) for the above values of b and γ; this allowed us to take u_R substantially below 1, and still observe a Σ-S wave combination.

In Fig. 8b, we have left u_L, b and γ the same, and increased u_R above $u = 1$. We now see the *same* undercompressive shock as in Fig. 8a, but now followed by a linear wave from u_+ to u_R. The solid curve has $u_R = 2$ and is monotone (modulo some nearly invisible undulation in the linear wave due to dispersion); the dashed curve has $u_R = 1.01 < u_+$ and is clearly nonmonotone. As in Fig. 8a, the two waves move apart. Specifically, the shock speed is $s = 0.455$ and the linear wave speed is $b = 0.75$. Note

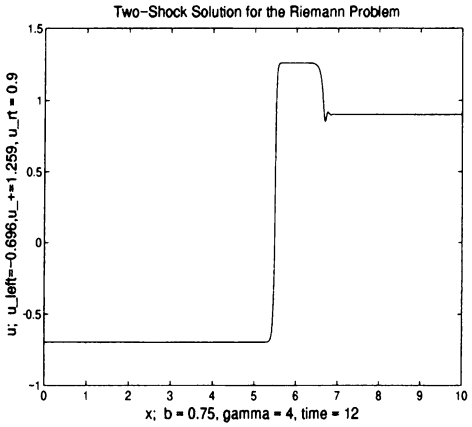

8a. $\Sigma - S$ solution:
$t = 12$, $u_R = 0.9$

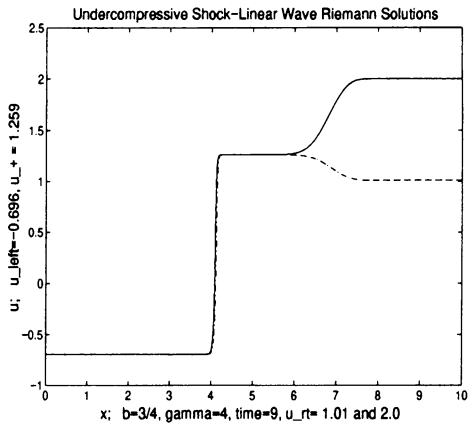

8b. $\Sigma - \mathcal{L}_b$ solutions
$t = 9$: $u_R = 2$ (solid), $u_R = 1.01$ (dashed).

FIG. 8. Numerical Riemann solutions with $u_L = -0.696, b = 0.75, \gamma = 4.0$

that while the runtimes of the two solutions in Fig. 8b were identical, and their states u_+ are indistinguishable, the shock locations are slightly separated. This fine separation could go back to the transition from initial data to Riemann solution, near $t = 0$. For the values of b and γ we tested, the linear waves exhibit some oscillation associated with the dispersion, but they are still very much like diffusion waves. Since diffusion waves are governed by the heat kernel, they spread out like $\sim \sqrt{t}$ for large t. In particular, the broad smoothing of the faster wave in Fig. 8b is due to dissipation in the partial differential equation, and not numerical effects.

Acknowledgment. This paper arose from discussions and preliminary calculations with Philippe LeFloch, and we would like to thank him for his contributions.

REFERENCES

[1] R. Abeyaratne and J. K. Knowles, *Implications of viscosity and strain gradient effects for the kinetics of propagating phase boundaries in solids*, SIAM J. Appl. Math. **51**, 1205–1221 (1991)
[2] B. T. Hayes and P. G. LeFloch, *Nonclassical shock waves: Scalar conservation laws*, Arch. Rat. Mech. Anal. **139**, 1–56 (1997)
[3] B. T. Hayes and P. G. LeFloch, *Nonclassical shock waves and kinetic relations: Finite difference schemes*, SIAM J. Numer. Anal. **35**, 2169–2194 (1998)
[4] B. T. Hayes and M. Shearer, *Undercompressive shocks and Riemann problems for scalar conservation laws with non-convex fluxes*, Proc. Royal Soc. Edinburgh Sect. A **129**, 733–754 (1999)
[5] E. Isaacson, D. Marchesin, and B. Plohr, *Transitional waves for conservation laws*, SIAM J. Math. Anal. **21**, 837–866 (1990)
[6] D. Jacobs, W. McKinney, and M. Shearer, *Travelling wave solutions of the modified Korteweg-de Vries-Burgers equation*, J. Differential Equations **116**, 448–467 (1995)
[7] P. D. Lax, *Hyperbolic systems of conservation laws* II, Comm. Pure Appl. Math. **10**, 537–566 (1957)
[8] A. Azevedo, D. Marchesin, B. Plohr, and K. Zumbrun, *Bifurcation of nonclassical viscous shock profiles from the constant state*, Comm. Math. Phys. **202**, 267–290 (1999)

[9] M. Schulze and M. Shearer, *Undercompressive shocks for a system of hyperbolic conservation laws with cubic nonlinearity*, J. Math. Anal. Appl. **229**, 344–362 (1999)

[10] M. Shearer and Y. Yang, *The Riemann problem for a system of conservation laws of mixed type with a cubic nonlinearity*, Proc. Royal Soc. Edinburgh Sect. A **125**, 675–699 (1995)

[11] M. Slemrod, *Admissibility criteria for propagating phase boundaries in a van der Waals fluid*, Arch. Rat. Mech. Anal. **81**, 301–315 (1983)

[12] C. C. Wu, *New theory of MHD shock waves*, Viscous Profiles and Numerical Methods for Shock Waves (ed. M. Shearer), SIAM, Philadelphia, PA, 1991, pp. 209–236